Interaction between Hopf and convective instabilities in a flow reactor with cubic autocatalator kinetics

Razvan Satnoianu,[1,2] John Merkin,[1] and Stephen Scott[2]
[1]*Department of Applied Mathematics, University of Leeds, Leeds LS2 9JI, United Kingdom*
[2]*School of Chemistry, University of Leeds, Leeds LS2 9JT, United Kingdom*
(Received 4 August 1997)

The interaction between Hopf and convective instabilities in a flow system based on cubic autocatalator kinetics is discussed. The interaction is described in terms of solutions to a complex Ginzburg-Landau equation. These solutions are wave packets consisting of regions of constant amplitude (and different phase) separated by a region of irregular behavior.
[S1063-651X(98)11303-X]

PACS number(s): 47.20.Ky, 03.40.Kf, 82.40.−g

The differential-flow-induced chemical instability (DIFICI) [1–3] has aroused considerable interest recently as a mechanism for producing spatial structure in chemical systems due to its inherent differences with the much more widely considered Turing instability. In part, this interest in the DIFICI is sustained by its experimental verification in a differential-flow reactor, a device in which some of the reagents required for the reaction are immobilized within the reactor while the rest are allowed to flow (and diffuse) freely. This highlights an important difference between the DIFICI and Turing mechanisms in that in the former case the spatial structures that arise propagate through the system whereas in the latter case the basic bifurcation is to steady, though spatially varying, behavior.

A model for this reactor, based on cubic autocatalator (or Gray-Scott) kinetics, has been considered in [4], where it was shown that the DIFICI arises essentially through a convective (or spatial) instability [5,6]. The model taken in [4] assumed that the substrate had been immobilized with the autocatalyst being made to flow. The spatially uniform steady state then became unstable at a critical (nonzero) flow rate. At higher flow rates a wave packet developed that consisted of waves of constant amplitude and frequency and that propagated through the system with a constant velocity growing in lateral extent as it did so, leaving the system in its original spatially uniform steady state at its rear. This model emphasizes a further difference between the DIFICI and Turing instabilities as the latter requires (for cubic autocatalator kinetics) that the autocatalyst be relatively immobile compared to the substrate [7,8], the opposite situation to the model in [4].

A feature of our flow-reactor model [4] is its ability to sustain spatially uniform temporal oscillations arising from a supercritical Hopf bifurcation as well as propagating spatial structures arising from convective instabilities. There is then the possibility of the interaction between these two mechanisms for destabilizing the spatially uniform steady state and this is what we consider. The linear stability analysis presented in [4] shows that the critical flow rate approaches zero as the Hopf bifurcation is approached. We exploit this, through a weakly nonlinear analysis valid close to the Hopf bifurcation and for small flow rates, to derive a complex Ginzburg-Landau equation (CGLE) to describe this two-mode interaction. The simplicity of our model enables this equation to be readily obtained, a clear identification between the behavior of the solutions to the CGLE (valid close to the mode interaction) and their counterparts in the original model is then possible. Thus our treatment complements that presented recently in [9], where a CGLE for a DIFICI-Hopf interaction was derived heuristically for a general system and where direct comparison with a specific model is not readily available. Further, the relative simplicity of the CGLE for our model permits a detailed examination, revealing complex spatiotemporal structures that were not seen in the more general treatment [9].

Our model is based on the reaction between substrate A and autocatalyst B with the kinetic scheme:

$$P \rightarrow A, \quad \text{rate} = \kappa_0[P]_0,$$
$$A + 2B \rightarrow 3A, \quad \text{rate} = \kappa_1[A][B]^2, \tag{1}$$
$$B \rightarrow \text{inert}, \quad \text{rate} = \kappa_2[B],$$

where the κ_i $(i=0,1,2)$ are constants. We assume that A is made immobile within the reactor and that B can flow with a constant velocity. With the further assumption of planar geometry we arrive at the dimensionless equations [4]

$$\frac{\partial a}{\partial t} = \mu - ab^2, \tag{2}$$

$$\frac{\partial b}{\partial t} = \frac{\partial^2 b}{\partial x^2} - \phi\frac{\partial b}{\partial x} + ab^2 - b \tag{3}$$

on $-\infty < x < \infty$, $t > 0$. Initially the system is in its spatially uniform steady state

$$a(x,0) = \mu^{-1}, \quad b(x,0) = \mu \tag{4}$$

with a small local perturbation being made to Eq. (4) at $t = 0$. In the above ϕ is the dimensionless flow rate (our bifurcation parameter) and μ is the dimensionless rate of production of A from the precursor P. Equations (2),(3) are derived in full in [4]. We note [10] that Eq. (4) is temporally stable for $\mu > 1$ and undergoes a supercritical Hopf bifurcation at $\mu = 1$ giving stable limit cycles in $\mu < 1$.

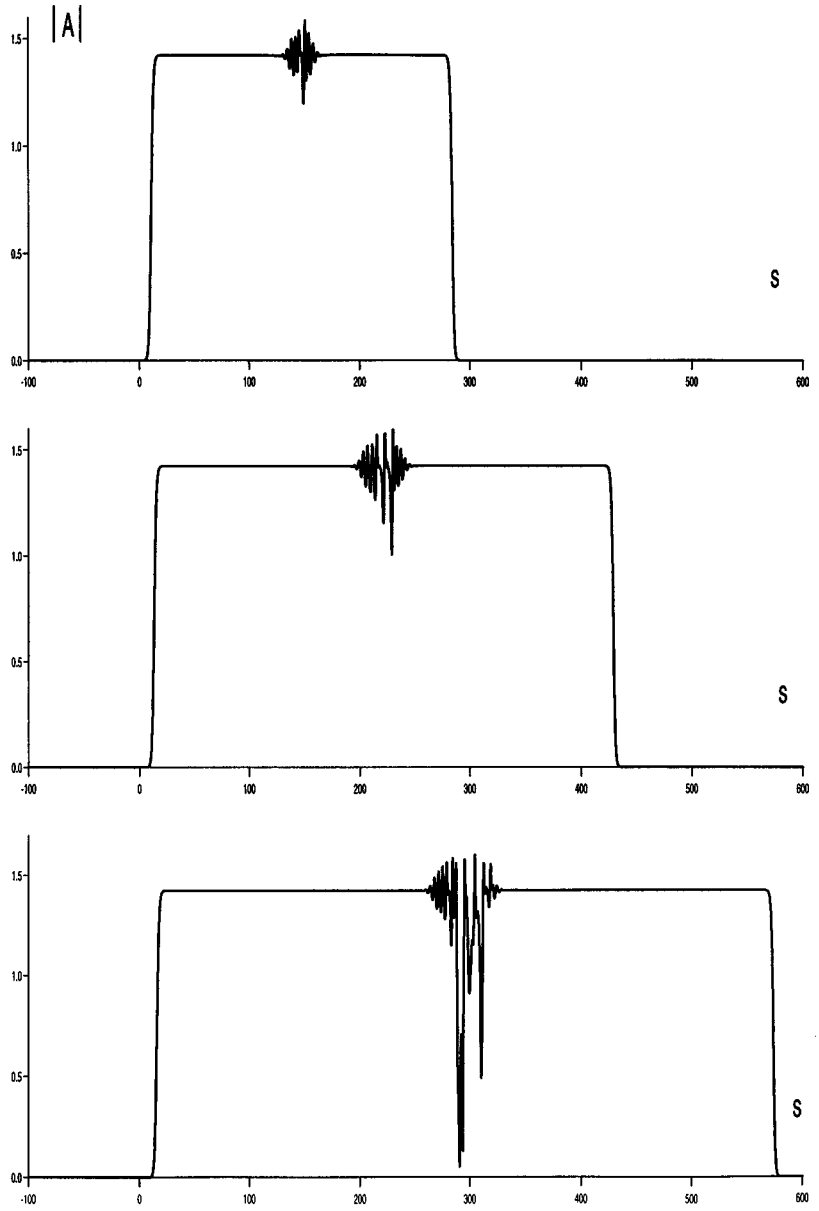

FIG. 1. Plots of the amplitude $|A|$ at equal time intervals obtained from a numerical integration of Eq. (10) for $\psi=3.0$. The system was perturbed initially in a small region centered on $s=0$.

In [4] it was shown that, for $\phi>\phi_c$, there is a range of wave numbers k for which steady state (4) is unstable to small local perturbations, where ϕ_c is the minimum on the neutral curve

$$\phi^2=\frac{(k^2+\mu^2-1)^2(k^2+1)}{k^2(1-k^2)}, \quad \mu>1, \quad 0<k<1. \tag{5}$$

Furthermore

$$\phi_c\sim 2\sqrt{2}(\mu-1)^{1/2}+\cdots \quad \text{as} \quad \mu\to 1^+. \tag{6}$$

To derive the CGLE describing the DIFICI-Hopf interaction for our model we put

$$\mu=1+r\epsilon^2, \quad 0<\epsilon\ll 1, \quad r=\pm 1 \tag{7}$$

with Eq. (6) suggesting that we scale

$$\phi=\epsilon\psi, \quad \psi=0(1) \quad \text{as} \quad \epsilon\to 0. \tag{8}$$

An expansion in powers of ϵ about the spatially uniform initial state (4), with an $0(\epsilon)$ term of the form

$$(a_1,b_1)=A(s,\tau)e^{it}(-2,1+i)+\text{c.c.}, \tag{9}$$

where s and τ are the long space and time variables, $s=\epsilon x$, $\tau=\epsilon^2 t$, leads, through the use of the method of multiple scales [11] to keep the expansion uniform by removing the secular terms that arise at $0(\epsilon^3)$, to the CGLE for the complex amplitude $A(s,\tau)$ as

$$\frac{\partial A}{\partial\tau}=\frac{(1-i)}{2}\frac{\partial^2 A}{\partial s^2}-\frac{\psi(1-i)}{2}\frac{\partial A}{\partial s}-r(1-i)A - \left(1+\frac{5i}{3}\right)A|A|^2 \tag{10}$$

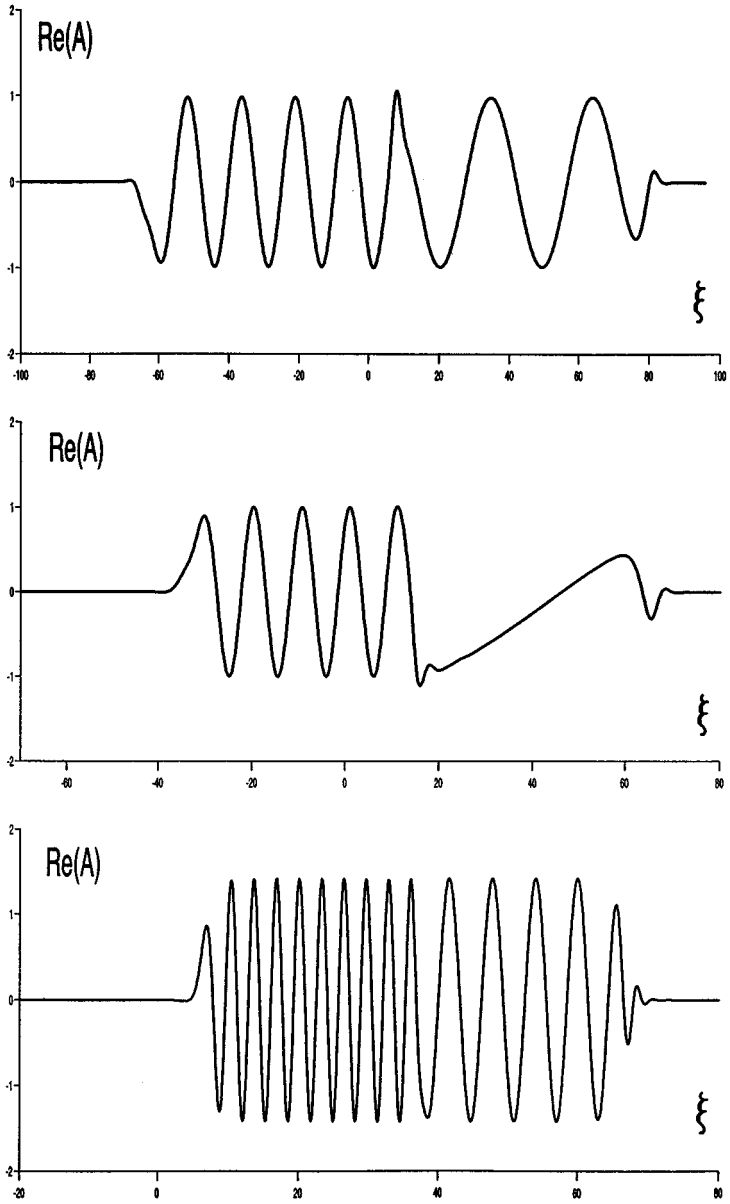

FIG. 2. Plots of Re(A) at large times for $\psi=0.2$, 0.573, 3.0.

on $-\infty<s<\infty$, $\tau>0$ with $A=0$ initially and subject to some local input.

We consider the case $\mu<1$ ($r=-1$) and start by discussing the linearized version of Eq. (10). If we look for a solution to this equation in the form $A(s,\tau)=A_s e^{\omega\tau-iks}$, where A_s is a constant, we obtain the dispersion relation

$$\omega(k)=-\frac{(1-i)}{2}k^2+\frac{(1+i)}{2}\psi k+(1-i). \tag{11}$$

Equation (11) shows that there are wave numbers for which $\mathrm{Re}(\omega)>0$ and to determine the nature of the ensuing instability we first need to find the saddle point (i.e., the values ω_s, k_s where $d\omega/dk=0$) for the estimation of the Fourier integrals for large τ. From Eq. (11) we find

$$k_s=\frac{i\psi}{2},\quad \mathrm{Re}(\omega_s)=1-\frac{\psi^2}{8}. \tag{12}$$

From Eqs. (11) and (12) it then follows that the unperturbed state ($A=0$) is absolutely unstable for $\psi<2\sqrt{2}$ and convectively unstable for $\psi>2\sqrt{2}$ (see [5,6]). The most unstable wave number is $k=\psi/2$, giving a group velocity,

$$v_g=\frac{d\ \mathrm{Im}(\omega)}{dk}=\psi \tag{13}$$

for this wave number.

If we now consider the linearized equation in a reference frame moving with (constant) velocity v, the equation for the frequency, now $\alpha(k)$, is modified to

$$\alpha(k)=\omega(k)-ikv \tag{14}$$

with corresponding saddle point at

$$k_s=\tfrac{1}{2}[i\psi+(1-i)v],\quad \mathrm{Re}(\alpha_s)=\tfrac{1}{8}(8-\psi^2+4\psi v-2v^2). \tag{15}$$

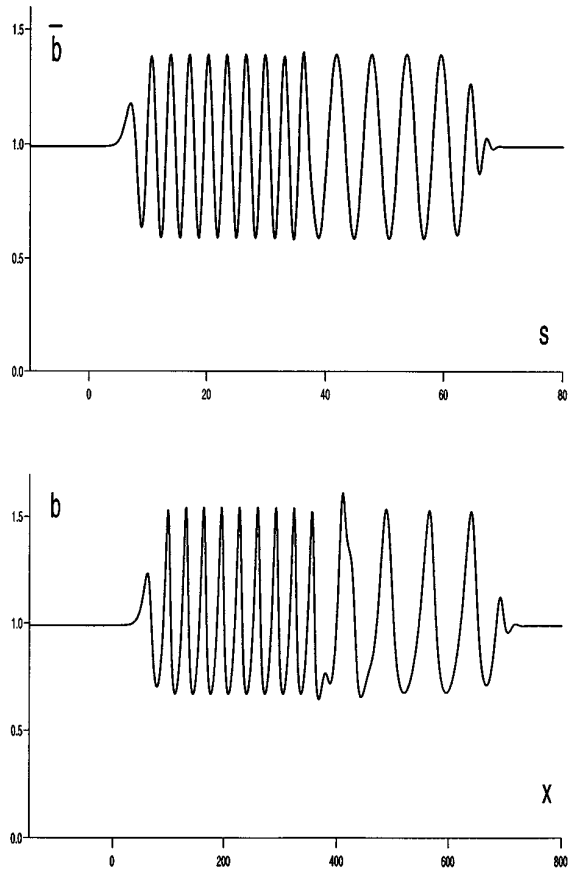

FIG. 3. Plots of the concentration b in the wave packet obtained (a) from the solution to the CGL equation (10) using Eq. (9) for $\psi=3.0$, (b) from a numerical solution to the initial-value problem (2),(3) for $\mu=0.99$, $\phi=0.3$.

At the edges of the wave packet we have neutral stability, i.e., $\mathrm{Re}(\alpha_s)=0$, which gives velocities, from Eq. (15),

$$v_{1,2}=\psi\pm\sqrt{4+\frac{\psi^2}{2}},\quad v_2>v_1. \tag{16}$$

The linear stability analysis suggests that solutions to Eq. (10) will be wave packets traveling with overall velocity $v_g=\psi$, with front and rear propagating with speeds $v_2>\psi$ and $v_1<\psi$, respectively. Note that $v_1<0$ if $\psi<2\sqrt{2}$ as expected. This is confirmed by numerical integrations of Eq. (10); we show a typical example, for $\psi=3.0$, in Fig. 1. Here the initial state $A=0$ was perturbed in a small region centered on $s=0$ and we plot the amplitude $|A|$ at equal time intervals starting after sufficient time had elapsed for the solution to develop fully. This figure (and integrations for other values of ψ) shows the front and rear of the wave packet propagating with different velocities, both of which are different from the propagation velocity of the wave packet itself. The computed values of these velocities correlate well with those predicted above by the linear analysis. For this value of ψ the system is only marginally convectively unstable and this can be observed by the rear of the wave packet propagating only very slowly forwards. A further feature to note is the establishment of two regions of constant amplitude separated by a region of irregular behavior, increasing slowly in extent and propagating with the group velocity (i.e., centered on $s=\psi\tau$).

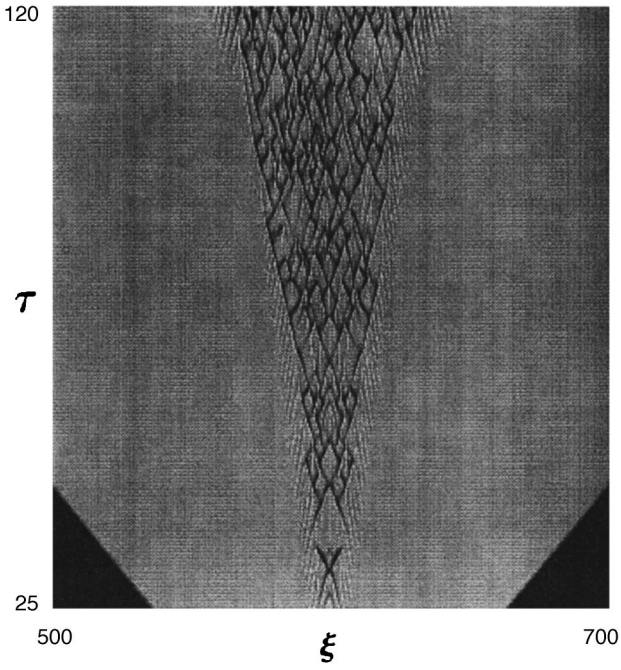

FIG. 4. Gray-level contour plot of $|A|$ for $\psi=3.0$ to illustrate the two regions of constant amplitude regular wave trains separated by a region of chaotic behavior. In this figure the darker the color the smaller the value of $|A|$.

We now consider the solution to the full Eq. (10). The above discussion suggests that a more appropriate variable to use is $\xi=s-\psi\tau$ and then to look for traveling wave solutions of the form

$$A=R_i\exp[i(k_i\xi-\omega_i\tau)],\quad R_i \text{ a real constant } (i=1,2) \tag{17}$$

in the front part ($i=2$) and rear part ($i=1$) of the wave packet. From Eq. (10) we obtain the relations

$$R_i^2=1-\frac{k_i^2}{2}-\frac{\psi k_i}{2},\quad \omega_i=\frac{4}{3}(2-k_i^2-\psi k_i). \tag{18}$$

To determine the k_i (and hence R_i and ω_i) in each region we require the wave solutions (17) to match with the solutions at the front and rear of the wave, where linear theory applies. This leads, after expressing Eq. (10) in terms of ξ and requiring neutral stability at the front and rear of the wave packet, to the relation

$$k_iu_i-\tfrac{4}{3}(2-k_i^2-\psi k_i)=-\tfrac{1}{8}(8+2v_i^2+4v_i\psi+\psi^2). \tag{19}$$

These terms arise from Eqs. (17) and (18) and from the linear theory when expressed in terms of $y=\xi-u_i\tau$, the variable appropriate to the propagating front and rear of the wave packet. For the front $u_2=\sqrt{4+\psi^2/2}$ and for the rear $u_1=-\sqrt{4+\psi^2/2}$, from Eq. (16) expressed in the moving frame. This then enables k_i, R_i, ω_i to be determined in terms of ψ.

Applying these expressions for u_1 and u_2 in Eqs. (18) and (19) shows that $k_1<0$ for all ψ and that $|k_1|$ increase as ψ increases. We find that k_2 changes sign at $\psi=\psi_0$, where $\psi_0^2=\frac{8}{3}(\sqrt{17}-4)$ ($\psi_0=0.57296$), with $k_2>0$ for $\psi<\psi_0$. At ψ_0 the wavelength of the waves forming the front part of the wave packet becomes infinite. Also at ψ_0, the direction of propagation (phase velocity) of the waves in the front part changes direction relative to that of the wave packet. A further important result to note is that $R_1=R_2$ for all ψ. Thus the waves in both the front and rear parts of the wave packet have the same amplitude though they have different frequencies (and phase velocities).

We illustrate these results in Fig. 2, where we plot large time profiles of Re(A) obtained from numerical integrations of Eq. (10) for $\psi=0.2$, 0.573, 3.0, these computations were done in the moving frame. Similar profiles are seen for Im(A). This figure shows the development of waves of different frequencies (though of the same amplitude; see also Fig. 1) in the front and rear parts of the wave packet and also the change in sign of the wave number at ψ_0. To assess the implications of this for the original initial-value problem (2),(3) we calculate the concentration b using Eq. (9) from our numerical solutions for A. Results from this are shown in Fig. 3(a) and compared with results obtained from the original system (2),(3) for $\mu=0.99$, $\phi=0.3$ [Fig. 3(b)].

A feature of our results is the region of irregular behavior separating the two regions of regular oscillations. This is particularly evident in Fig. 4, where we give a gray-level contour plot $|A|$ for $\psi=3.0$ started after the initial development shown in Fig. 1. This figure shows the region of irregular behavior expanding with time. Various tests were applied to the data in this region, including determining the spatial correlation function and an initial condition sensitivity analysis. These lead us to conclude that the behavior in this central region is a form of spatiotemporal chaos.

Finally, we mention briefly the behavior when $r=1$ ($\mu>1$). In this case the unperturbed state $A=0$ is globally stable for $\psi<2\sqrt{2}$ and convectively unstable for $\psi>2\sqrt{2}$. Again a two-frequency, constant amplitude wave structure develops with front and rear propagating with speeds $\psi\pm\sqrt{\psi^2/2-4}$ when the system is convectively unstable. The frequencies are ψ dependent, though now there is no possibility of these becoming zero. This behavior is in accord with that described in [4] for the original model.

[1] A. B. Rovinsky and M. Menzinger, Phys. Rev. Lett. **69**, 1193 (1992).
[2] A. B. Rovinsky and M. Menzinger, Phys. Rev. Lett. **70**, 778 (1993).
[3] M. Menzinger and A. B. Rovinsky, in *Chemical Waves and Patterns*, edited by R. Kapral and K. Showalter (Kluwer, Dordrecht, 1995).
[4] R. A. Satnoianu, J. H. Merkin and S. K. Scott, Physica D (to be published).
[5] R. J. Deissler, J. Stat. Phys. **40**, 371 (1985).
[6] R. J. Deissler, J. Stat. Phys. **54**, 1459 (1989).
[7] D. J. Needham and J. H. Merkin, Dyn. Stab. Syst. **4**, 259 (1989).
[8] R. Hill, J. H. Merkin and D. J. Needham, J. Engng. Math. **29**, 413 (1995).
[9] A. B. Rovinsky, A. Malevanets, and M. Menzinger, Physica D **95**, 306 (1996).
[10] J. H. Merkin, D. J. Needham, and S. K. Scott, SIAM (Soc. Ind. Appl. Math.) J. Appl. Math. **47**, 1040 (1987).
[11] A. H. Nayfey, *Perturbation Methods* (Wiley, New York, 1973).